Single-Cell RNA Sequencing Analysis of the Early Postnatal Mouse Lens Epithelium

Adrienne A. Giannone,[1] Caterina Sellitto,[1] Barbara Rosati,[1,2] David McKinnon,[3] and Thomas W. White[1]

[1]Department of Physiology and Biophysics, Stony Brook University School of Medicine, Stony Brook University, Stony Brook, New York, United States
[2]Veterans Affairs Medical Center, Northport, New York, United States
[3]Department of Neurobiology and Behavior, Stony Brook University School of Medicine, Stony Brook University, Stony Brook, New York, United States

Correspondence: Thomas W. White, Department of Physiology and Biophysics, Stony Brook University School of Medicine, Stony Brook University, T5-147, Basic Science Tower, Stony Brook, NY 11794-8661, USA;
thomas.white@stonybrook.edu.

Received: August 14, 2023
Accepted: October 6, 2023
Published: October 23, 2023

Citation: Giannone AA, Sellitto C, Rosati B, McKinnon D, White TW. Single-cell RNA sequencing analysis of the early postnatal mouse lens epithelium. *Invest Ophthalmol Vis Sci.* 2023;64(13):37.
https://doi.org/10.1167/iovs.64.13.37

Purpose. The lens epithelium maintains the overall health of the organ. We used single-cell RNA sequencing (scRNA-seq) technology to assess transcriptional heterogeneity between cells in the postnatal day 2 (P2) epithelium and identify distinct epithelial cell subtypes. Analysis of these data was used to better understand lens growth, differentiation, and homeostasis on P2.

Methods. scRNA-seq on P2 mouse lenses was performed using the 10x Genomics Chromium Single Cell 3′ Kit (v3.1) and short-read Illumina sequencing. Sequence alignment and preprocessing of data were conducted using 10x Genomics Cell Ranger software. Seurat was employed for preprocessing, quality control, dimensionality reduction, and cell clustering, and Monocle was utilized for trajectory analysis to understand the developmental progression of the lens cells. CellChat and GO analyses were used to explore cell–cell communication networks and signaling interactions.

Results. Lens epithelial cells (LECs) were divided into seven subclusters, classified by specific gene markers. The expression of crystallin, cell-cycle, and metabolic genes was not uniform, indicating distinct functional roles of LECs. Trajectory analysis predicted a bifurcation of differentiating and cycling cells from an *Igfbp5*+ progenitor pool. We also identified heterogeneity in signaling molecules and pathways, suggesting that cycling and progenitor subclusters have prominent roles in coordinating crosstalk.

Conclusions. scRNA-seq corroborated many known markers of epithelial differentiation and proliferation while providing further insight into the pathways and genes directing these processes. Interestingly, we demonstrated that the developing epithelium can be divided into distinct subpopulations. These clusters reflect the transcriptionally diverse roles of the epithelium in proliferation, signaling, and maintenance.

Keywords: mouse, lens development, single-cell sequencing, postnatal day 2

The anterior surface of the eye lens is covered by a monolayer epithelium that provides the sustenance, coordinated transport, and communication that the lens requires for growth and development and to maintain its optical properties.[1,2] In addition, these epithelial cells must differentiate into fibers cells at the lens equator that express high levels of crystallin protein to provide the high refractive index required to focus images on the retina.[3] During development, epithelial cells undergo proliferation to provide new cells destined for the fiber differentiation pathway and new epithelial cells for the growing surface area of the lens.[4,5] Furthermore, the non-proliferating epithelial cells have well established and spatially segregated metabolic and transport functions.[6,7] Although derived from a common origin, lens epithelial cells fulfill a variety of specialized functions to maintain the developmental and homeostatic needs of the growing lens.

Lens epithelial cell (LEC) proliferation is dependent on growth factor responses. Specifically, fibroblast growth factor (FGF) induction of mitogen-activated protein kinase/extracellular regulated kinase 1/2 (MAPK/ERK1/2) and the phosphoinositide 3-kinase (PI3K)/Akt signaling pathways have been implicated in epithelial proliferation, migration, and differentiation decisions.[8,9] FGF-induced responses in LECs depend on fibroblast growth factor receptors (FGFRs) and subsequent downstream signaling events. In embryonic and early postnatal mouse lenses, LEC proliferation occurs across the anterior epithelium, with the highest levels near the equator.[10,11] In older rodent lenses, LEC proliferation is concentrated in a specific area of the epithelial monolayer, located just anterior to the equatorial region, referred to as the germinative zone.[5,12]

There is a significant increase in LEC proliferation during the first postnatal week of life in mice, which is crucial

for the overall growth of the organ. There is a transitory spike in proliferation at postnatal day 2 (P2) followed by a reduction through P7.[10,11] This early oscillating rise in cellular proliferation correlates to cell-cycle phases and is important for maintaining the lifelong integrity and structure of the lens.[13,14] In order to characterize the different LEC transcriptional states and to probe potential subpopulations that underscore this critical proliferative event, we utilized single-cell RNA sequencing (scRNA-seq) technology. Previous single-cell RNA sequencing studies in the lens have been conducted in zebrafish,[15,16] human,[17–19] *Drosophila*,[20] chick,[21] and adult murine lenses.[22] However, the early postnatal mouse lens epithelium has not yet been characterized using this method.

Probing the cellular heterogeneity of LECs and understanding the cell–cell communication networks that underlie proliferation, differentiation, and metabolism are critical for understanding overall lens physiology and homeostasis. In this study, we performed scRNA-seq on P2 mouse lenses. Our analysis identified seven subpopulations within P2 LECs that had transcriptionally distinct states. These subpopulations could be further classified into three broader categories: progenitor, cycling, or differentiating cells. Based on known markers of lens differentiation and trajectory analysis, we modeled the differentiation trajectory of LECs and were able to identify the associated genes that were potentially contributing. We also identified differential cell–cell communication networks and signaling pathways engaged in earlier versus later cell states and showed the possible heterogeneity of signaling within LEC subpopulations. This work provides valuable insights into LEC transcriptional organization and lays the foundation for future studies to characterize subpopulations, identify disease states, and interpret key signaling and transcription events in the lens epithelium.

Methods

Cell Isolation

Single LECs for RNA sequencing were isolated from P2 wild-type C57BL/6N pups (Taconic Biosciences, Germantown, NY, USA) following an approved Institutional Animal Care and Use Committee protocol and adhering to the ARVO Statement for the Use of Animals in Ophthalmic and Vision Research. Two independent pools of P2 LECs were generated and analyzed. Lenses were dissected from 4 to 8 mouse pups in Tyrode's solution on a warm stage (37°C). Lenses were first cleaned of the ciliary body and tunica vasculosa using fine forceps, then by digestion in 0.05% trypsin-EDTA for 10 minutes at 37°C and 5% CO_2. After transfer to ice-cold Tyrode's solution for 10 minutes, the lens capsule with the adhering epithelial monolayer was peeled off the remaining fiber cell mass using fine forceps and transferred to a tube containing 100 µL of $Ca^{2+}Mg^{2+}$-free Dulbecco's phosphate-buffered saline (DPBS; Thermo Fisher Scientific, Waltham, MA, USA) on ice. When all capsules were collected, the tube was moved to 37°C, and 100 µL of 0.1% Collagenase/Dispase Blend (MilliporeSigma, Burlington, MA, USA) was added. After 5 minutes, 1 mL of 0.5% trypsin-EDTA (Thermo Fisher Scientific) was added, and the capsule mass was gently triturated by pipetting, transferred into a culture dish, and trypsinized at 37°C and 5% CO_2. Trypsinization was monitored under a dissecting microscope until the majority of cells were present as single cells. Minimum Essential Medium (MEM; Thermo Fisher Scientific) supplemented with 10% fetal bovine serum and antibiotics was added, and cells were centrifuged for 5 minutes at 230 relative centrifugal force. The cell pellet was washed once by centrifugation at 4°C in DPBS containing 0.04% RNase-free bovine serum albumin (BSA) (MilliporeSigma). The final pellet was resuspended in the appropriate volume of DPBS/0.04% RNAse-free BSA to have a cell density of 1500 to 2500 cells per microliter and filtered using a 20-µm cell mini-strainer (PluriSelect, Leipzig, Germany). Freshly isolated cell suspensions were immediately processed in the 10x Genomics workflow as described below.

Single-Cell Sequencing

The scRNA-seq libraries were generated using the Single Cell 3′ Reagent Kit v3.1 (10x Genomics, Pleasanton, CA), according to the manufacturer's instructions. Briefly, cells, gel beads, and partitioning oil were loaded onto a Chromium Next GEM Chip G, for a target recovery of 10,000 cells per sample. The chip was processed in a Chromium Controller (10x Genomics) to generate Gel Beads-in-emulsion (GEMs). After reverse transcription using a GEM–reverse transcription (RT) incubation protocol on a PCR cycler, the GEMs were broken using Recovery Agent (10x Genomics), and the cDNA was purified with DynaBeads MyOne Silane beads (10x Genomics), amplified with PCR for 11 cycles, and further purified with SPRIselect magnetic beads (Beckman Coulter, Brea, CA, USA). Quality control and quantification of recovered PCR products were performed on a TapeStation 4200 with the Agilent High Sensitivity D5000 ScreenTape System (Agilent, Santa Clara, CA, USA). The scRNA-seq libraries were generated using 25% of the cDNA yield (10 µL). After fragmentation, end repair, A-tailing, and size selection purification, the cDNA was ligated with adaptors and purified again with SPRISselect beads. Libraries were amplified using PCR with sample index oligonucleotides from the Chromium i7 Multiplex Kit (10x Genomics), for a total of 10 or 11 PCR cycles, as estimated from the initial cDNA input. The final PCR products were subjected to double-sided size selection with SPRISselect beads (0.6× and 0.8×). Library quality control was performed on the Agilent TapeStation 4200, and the library yield was quantified by quantitative PCR (qPCR) using the KAPA Library Quantification Kit (Roche Diagnostics, Indianapolis, IN, USA). Sequencing was performed through a commercial supplier (Novogene, Durham, NC, USA) at a depth of 20,000 paired reads per cell on an Illumina NovaSeq 6000 sequencer with the following (PE150) sequencing settings: Read 1, 151 cycles; i7 index, 8 cycles; Read 2, 151 cycles.

Preprocessing, Quality Control, Clustering, Integration, and Cell-Type Identification

Raw data were aligned to the mouse genome (mm10) reference transcriptome and underwent preprocessing with Cell Ranger 6.1. The count matrix was then analyzed using Seurat 4.3.0 (R Foundation for Statistical Computing, Vienna, Austria).[23] Filtering included removal of cells in the bottom 2% and upper 3% of expressed genes (nGene) and expressed RNA (nUMI) fractions and removal of cells with more than 15% mitochondrial reads. Approximately 8% of the droplets were identified as containing multipets by DoubletFinder[24]

and were removed from further analysis (Supplementary Figs. S1, S2).

Normalization was performed using SCTransform followed by regression of cycle genes. The two independent samples were integrated with Harmony.[25] Dimensionality reduction was performed using principal component analysis and Uniform Manifold Approximation and Projection (UMAP). Clustering was performed using the Louvain algorithm. Canonical gene markers were used to identify four unique cell types within 11 cell subpopulations.

After this initial analysis, the LECs were identified and subset for further analysis. Gene set enrichment was performed using the clusterProfiler and Fast Gene Set Enrichment Analysis (fgsea) R packages. The results of the Gene Ontology (GO), Reactome, and Hallmark pathway analysis were filtered using a Benjamini–Hochberg (BH)-adjusted $P < 0.05$ and sorted by normalized enrichment score (NES) magnitude.

Cell Trajectory and Pseudotime Analysis

Pseudotime modeling was performed using Monocle 3 (v1.3.1).[26] Trajectories were identified and cells ordered based on pseudotime using the learn_graph function and visualized using the plot_cells function, respectively. The Progenitor cluster (cluster 0) was used as the root cluster. For downstream analysis, estimate_size_factors was first used to normalize gene expression, and then graph_test was run to look at differential gene expression throughout pseudotime. Gene modules were then identified using the find_gene_modules function, which utilizes the output of the graph_test function to group genes together based on their variance patterns along pseudotime. Gene outputs from the top two gene modules for each Seurat cluster were then classified using GO pathway analysis and submitted to PantherDB.org.[27]

Cell Communication Analysis

In order to quantify and visualize cell signaling and communication networks within LECs, CellChat 1.6.1 was utilized using the standard pipeline.[28] The entire CellChat database was used to analyze known ligand–receptor interactions between LECs and identify signaling pathways that may be present in LEC subpopulations.

Results

Identification of Cell Types in the P2 Mouse Lens

Two independent samples of freshly isolated P2 LECs were obtained from wild-type mice and analyzed using scRNA-seq. Cell types were manually identified based on the expression of canonical gene markers. This analysis suggested the presence of eight contiguous clusters of lens epithelial cells (clusters 0–7), and three single small clusters of endothelial cells (cluster 8), mural cells (cluster 9), and macrophages (cluster 10) (Fig. 1A). The majority (96.6%) of filtered cells were determined to be LECs (Fig. 1B). LEC identity (Fig. 1C) was inferred from high expression of known marker genes for this cell type, including the abundant crystallins *Cryaa* (αA crystallin) and *Cryab* (αB crystallin),[29] as well as *Gja8* (connexin 50).[30–34] Endothelial cells (Fig. 1D) were characterized by *Cldn5* and *Ctla2a* expression. *Cldn5* is abundantly expressed in microvascular endothelial cells, and *Ctla2a* is a capillary endothelial marker.[35,36] Mural cells (Fig. 1E) were categorized by expression of the marker genes *Rgs5* and *Serpine2*, which are vascular maturation and calcification factors, respectively.[37,38] Macrophages (Fig. 1F) were detected by expression of the complement system gene *C1qa*, as well as *Apoe*.[39,40] Within the identified LEC groups, cluster 7 was anomalous based on low median genes per cell, low median unique molecular identifier (UMI) counts per cell, a low percentage of mitochondrial RNAs, and a high percentage of ribosomal RNAs (Supplementary Fig. S2). These cells were assumed to be damaged, or stressed, and were removed from further downstream analysis.

LEC Subtypes Displayed Differential Gene Expression

Following annotation of cell types within the complete sample, LECs were subset and re-clustered (Fig. 2A). Approximately 33% of LECs were scored as cycling, with 14% in the G2M phase and 19% in the S phase (Fig. 2B). Among the seven identified LEC clusters remaining after subsetting, there was considerable heterogeneity of gene expression (Fig. 2C). In cluster 0, there was high expression of nutrient-responsive genes, such as the insulin-like growth factor (IGF) binding protein *Igfbp5*, the nutrient binding proteins *Slc7a11* and *Folr1*, and the neurogenic factor *Cntf* (Figs. 2C, 2D). *Igfbp5* is an IGF binding factor that plays a role in insulin signaling and early postnatal lens development and is regulated by *Pax6*.[41] IGF signaling in the lens also mediates proliferation, differentiation, and migration decisions during development.[42] *Slc7a11* is an amino acid transporter that has roles in growth and metabolism and is present in both LECs and lens fiber cells (LFCs) in zebrafish.[15] *Slc7a11* is a cystine/glutamate transporter that is involved in redox homeostasis by regulating intracellular glutathione (GSH) levels.[43] GSH is an essential antioxidant in the lens for maintaining optical lens clarity.[44] *Folr1* is a folate receptor that mediates the uptake of folate from the bloodstream, which is crucial for proper lens development.[45] GO analysis was used to functionally annotate the genes upregulated in cluster 0. This analysis showed that these genes had roles in cellular morphogenesis, epithelial maturation, collagen secretion, and IGF signaling (Fig. 3). This analysis identified several other signal pathway genes upregulated in cluster 0, including the bone morphogenetic protein (BMP) antagonist *Sostdc1*, the epithelial cell development factor *Klf4*, the cysteine protease *Ctsl*, the Wnt co-receptor *Fzd2*, *Tfap2a* (AP-2a), and the transforming growth factor (TGF) signaling factor *Tgfb2*. Specific collagen genes, such as *Pcolce*, were also upregulated in this cluster. Given the established roles of these differentially expressed genes, as well as the predominant G1 cell cycle state, this cluster was labeled the "progenitor" cluster.

In contrast, cell cluster 1 expressed many genes important for lens biology, such as *Cdkn1c*, *Ccdc80*, and *Adamtsl4*. *Cdkn1c* (also known as $p57^{Kip2}$) expression is a key marker of LEC cell cycle exit and initiation into differentiation.[46] The gene *Ccdc80* has strong homology to equarin, which is also a mediator of LEC differentiation in chick embryos.[47] *Thbs1* (thrombospondin) and *Id1* are both involved in mediating TGF-β signaling and activation in the lens.[48,49] *Adamtsl4* has a proposed role of anchoring zonular fibers to the lens equatorial region.[50] Enriched GO terms in this cluster included genes mainly involved in ribosome biosynthesis and

Investigative Ophthalmology & Visual Science

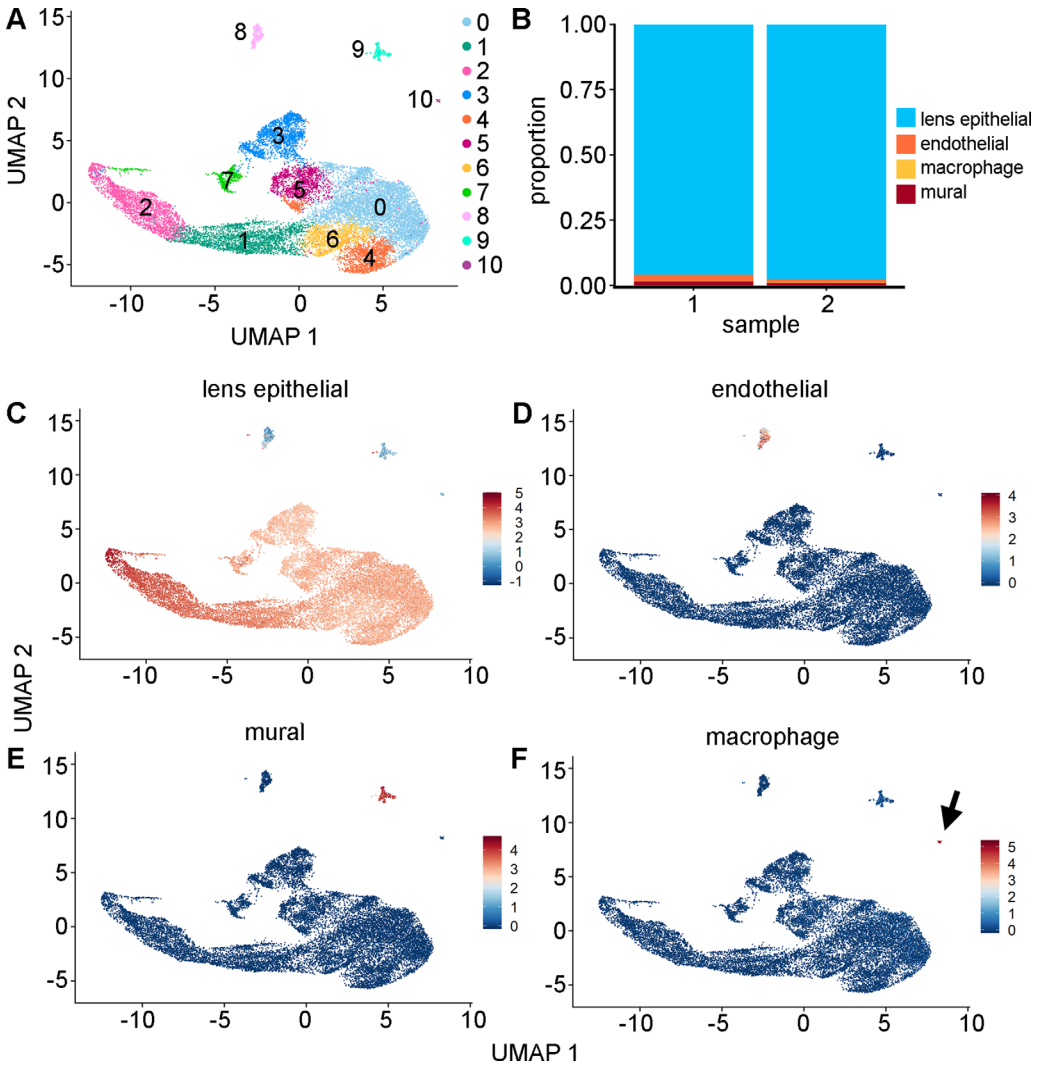

Figure 1. (**A**) In this study, 18,776 post-filtered cells were combined from two independent biological samples and visualized using a UMAP representation. To allow initial assessment of biological variation, the number of genes, number of transcripts, and mitochondrial and ribosomal RNA counts were not regressed out as sources of variation. In this analysis, the Louvain algorithm (resolution = 0.3) identified 11 clusters. (**B**) Proportion of cell-type numbers based on identified cell types for each of the two samples. Cell types were identified based on average expression of canonical gene markers for the four main cell types: (**C**) lens epithelial cells (*Cryaa*, *Cryab*, *Gja8*); (**D**) endothelial cells (*Cldn5*, *Col18a1*, *Ctla2a*); (**E**) mural cells (*Rgs5*, *Mgp*, *Serpine2*); and (**F**) macrophages (*Pf4*, *C1qa*, *Apoe*). The macrophage cluster is indicated by an *arrow*.

translation. An increase in ribosomal production could indicate translation of genes necessary for differentiation, especially given the co-expression of *Cdkn1c* in this cluster.[51] Ribosomal RNA production is highly enriched at the lens transitional zone.[52] Differentially expressed genes identified by GO terms included *Rbm24*, which plays a role in crystallin mRNA translation and LEC terminal differentiation, and the laminin gene *Lama2*.[53] Given the expression of genes involved in cell-cycle exit and initiation into differentiation, this cluster was identified as the "early differentiation" cluster.

Cluster 2 displayed abundant expression of beta and gamma crystallin genes, such as *Cryba2*, indicating that this cluster may contain cells further along the differentiation pathway than cluster 1.[54] Additionally, there was marked expression of *Cd24a*, which is a cell membrane adhesion protein known to be highly expressed in LFCs.[55] Expression of gamma crystallins starts to accumulate during epithelial elongation in cells located posteriorly to the equatorial region, as does *Crybb1*.[56] Crystallin expression may be temporally distinct, with gamma and beta crystallins specifically expressed later in the process of differentiation.[57] Additional cluster 2 genes associated with GO terms were mainly crystallin genes, but we also identified an increase in *Aqp0/Mip* (major intrinsic protein) expression in this cluster, as well as *Maf* (c-Maf), *Nbs*, *Bfsp1* (filensin), and *Lim2* (lens intrinsic membrane protein 2). The cells in this cluster had upregulation of genes related to fiber cell differentiation; therefore, this cluster was labeled the "late differentiating" cluster.

Cells in cluster 3 had cell-cycle scores predominantly in the G2/M and S phases and had distinct and unique expression of many histone-related genes, such as *Hist1h1b*, *Hist1h2ap*, and *Hist1a2ae*. Histone genes are transcribed throughout the cell cycle, with a large increase in histone mRNA levels during the S phase followed by selective

Investigative Ophthalmology & Visual Science

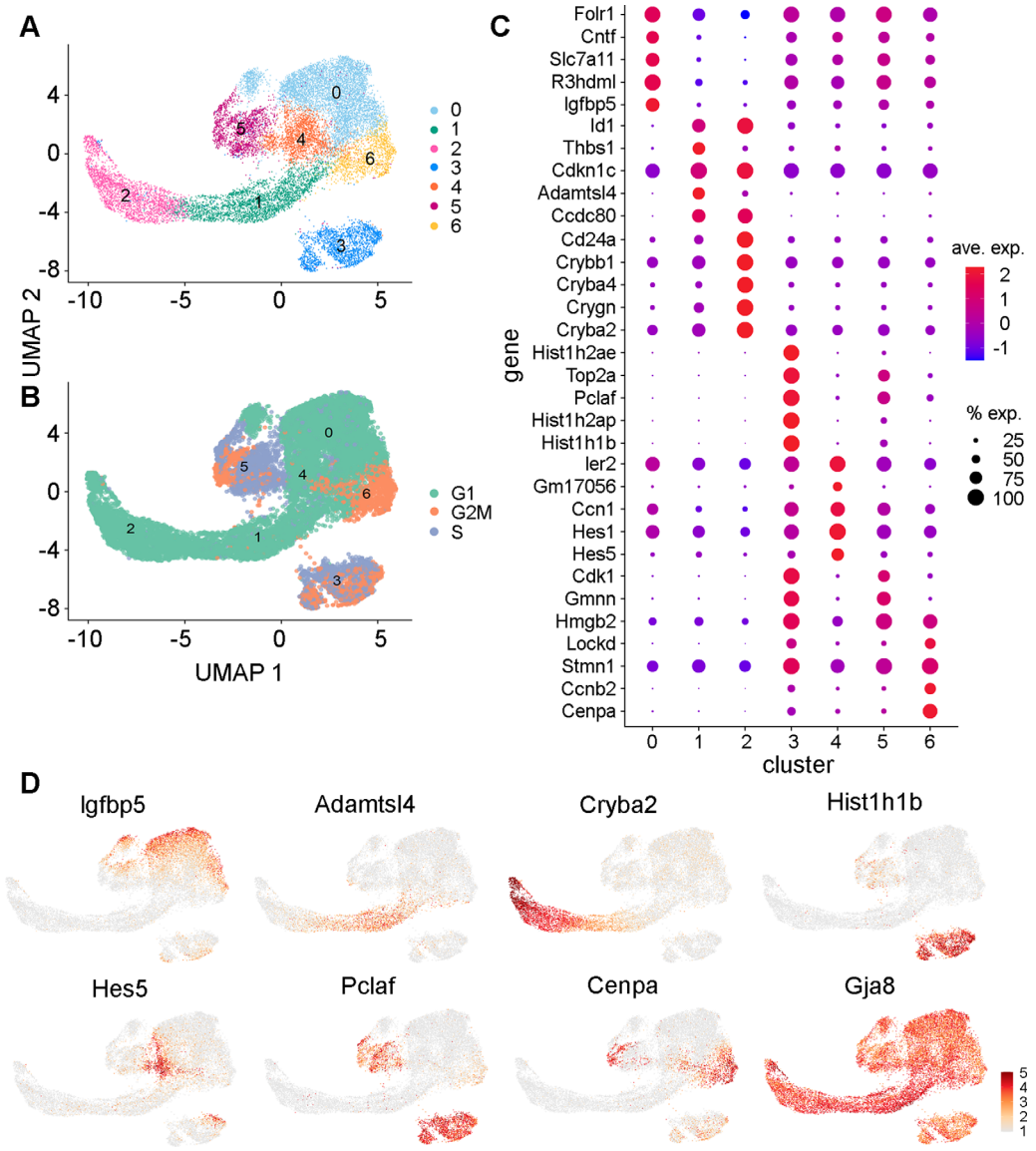

Figure 2. (**A**) UMAP representation of LECs after removal of other cell types and damaged cells. Lovain clustering (resolution, 0.2) identified seven subtypes. (**B**) Cell-cycle scores for each cluster. (**C**) Dot plot showing the top five differentially expressed genes for each of the seven LEC clusters. Duplicated markers are only shown once. (**D**) Examples of patterns of cluster-specific gene expression for seven selected marker genes and one ubiquitously expressed gene (*Gja8*).

degradation at the completion of DNA replication.[58] Histone posttranslational modifications and chromatin remodeling have important roles in lens development and LEC differentiation.[59,60] Mutations in histone genes, such as *Hist2h3c1*, have also been linked to cataract formation and an observed decrease in crystallin and *Aqp0* expression during development.[61] In crystallin-deficient lenses, the relative ratios of histones H2A/H2B and H3/H4 are altered, suggesting a synergistic relationship between crystallins and histones.[62] However, the relative abundance and roles of these histones in LEC subpopulations have yet to be established. Cluster 3 also displayed expression of *Pclaf*, which plays an essential role in cell proliferation but has not yet been described in the lens.[63] The GO analysis primarily identified an increase in cell cycle genes. Other differentially expressed genes identified by the GO analysis included the cell-cycle regulators *Fbxo5* and *Dbf4*. Based on these observations, cluster 3 was labeled the "Histone" cluster.

For cells in cluster 4, there was upregulated expression of the Notch effectors *Hes5* and *Hes1*. Notch signaling directly suppresses *Cdkn1c* in the lens epithelium and maintains a population of proliferating LECs.[46] During development, Notch effectors and recipients in LECs have spatially distinct expression that helps coordinate the decision to differentiate or proliferate.[64] The GO analysis identified that genetic markers of this cluster may be involved in Janus kinase (JAK)/signal transducer and activator of transcription (STAT) and tumor necrosis factor A (TNFA)/nuclear factor kappa B (NF-κB) signaling. Differentially expressed genes identified by GO analysis included *Socs3*, *Junb*, *Zfp36*, and *Fos/Jun* (AP-1). Due to the distinctive *Hes5/Hes1* expression, cluster 4 was labeled the "Notch Effector" cluster.

Investigative Ophthalmology & Visual Science

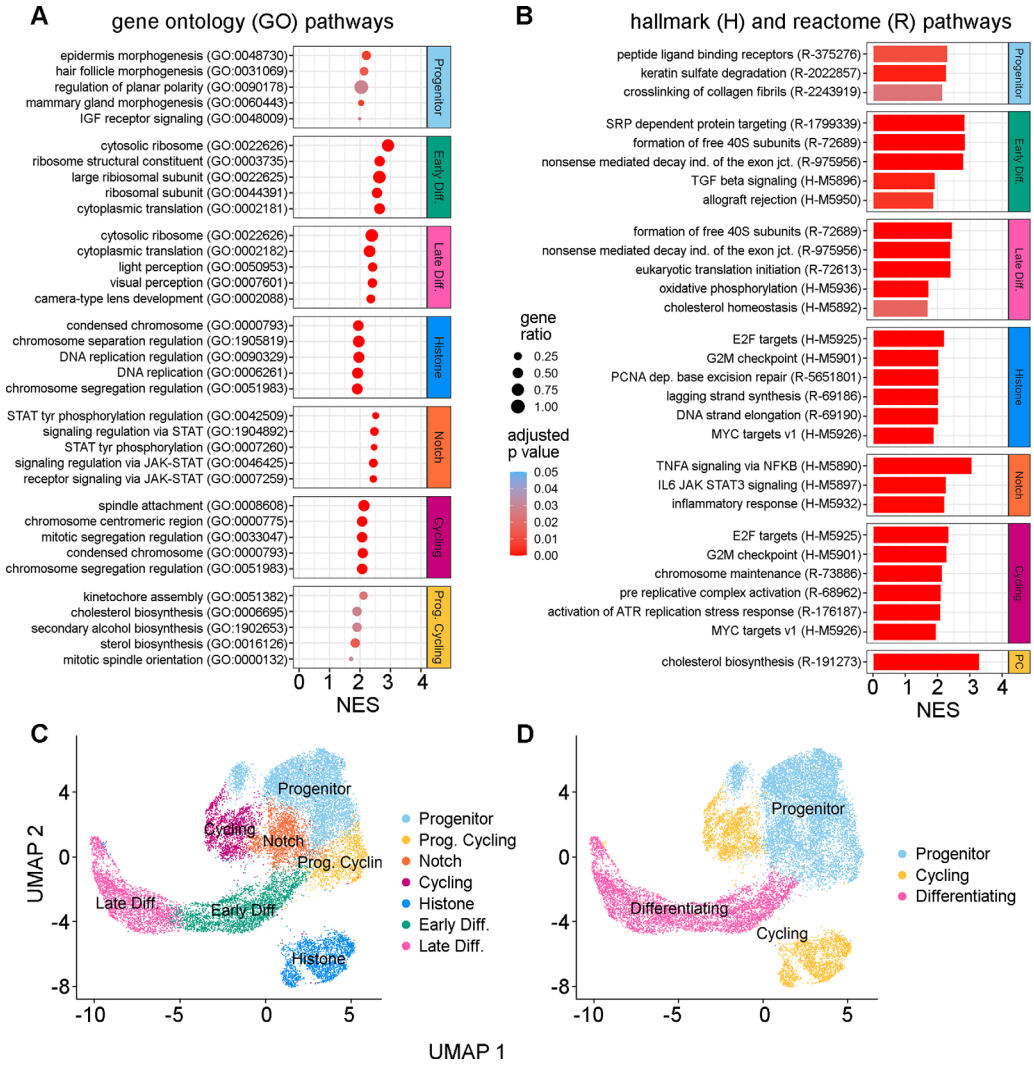

Figure 3. (**A**) GO term enrichment analysis. Only the top ($n = 5$) significant (adjusted $P < 0.05$) and upregulated (NES > 0) annotations per cluster are shown and ordered by NES magnitude. *Dot color* represents the adjusted *P* value intensity, and the *dot size* represents the gene ratio. (**B**) Reactome and Hallmark pathway enrichment. The top significant (adjusted $P < 0.05$) Reactome ($n = 3$) and Hallmark ($n = 3$) pathways are shown and ordered by NES magnitude. Some clusters did not have multiple significant pathways. *Scale bar intensity* reflects the adjusted *P* value. (**C**) Seven identified clusters are shown in a UMAP representation. (**D**) Three higher level groups are shown in a UMAP representation.

Cluster 5 contained cells in the G2M and S phases of the cell cycle and expressed several markers of cycling cells. This cluster had marked expression of *Cdk1* and *Gmnn*. *Cdk1* is an essential cell-cycle gene that controls progression through mitosis and is rarely expressed in post-mitotic cells.[65] *Gmnn* (geminin) is an S-phase regulator that also associates with chromatin.[66] Cluster 5 also had elevated expression of *Pclaf*, which is a cell-cycle regulator.[63] As these genes are key for cell-cycle progression, this cluster was labeled the "Cycling" cluster.

Cluster 6 contained cells primarily in the G2M phase that expressed genes more similar to the Progenitor cluster cell population than the other cycling clusters. Unique markers of this cluster included *Ccnb2* and *Cenpa*. *Ccnb2* (cyclin B2) has known function in LEC mitosis and is also expressed during terminal fiber cell differentiation.[67] *Cenpa* is a structural centromeric protein that also functions in nucleosome formation and regulation of chromatin.[68] GO analysis uniquely identified an upregulation of sterol and alcohol biosynthesis in this cluster, indicating that metabolic pathways may be present. Some genes identified from the GO analysis were *Fdps*, *Hmgcs1*, and *Msmo1*. These genes have been previously identified in the lens as regulators of cholesterol biosynthesis.[69] Interestingly, these biosynthetic genes were also upregulated in the Late Differentiating cluster. Given the similarities to progenitor cells and their biosynthetic properties, this cluster was labeled "Progenitor Cycling."

The relationship among these seven identified gene clusters was plotted in a UMAP representation (Fig. 3C). Based on hierarchical analysis of gene expression patterns, as well as the analysis of gene modules described below using Monocle (Supplementary Figs. S3B, S3C), it appeared likely that these clusters could also be grouped into three main classes: progenitor cells, cycling cells, and differentiating cells (Fig. 3D).

Investigative Ophthalmology & Visual Science

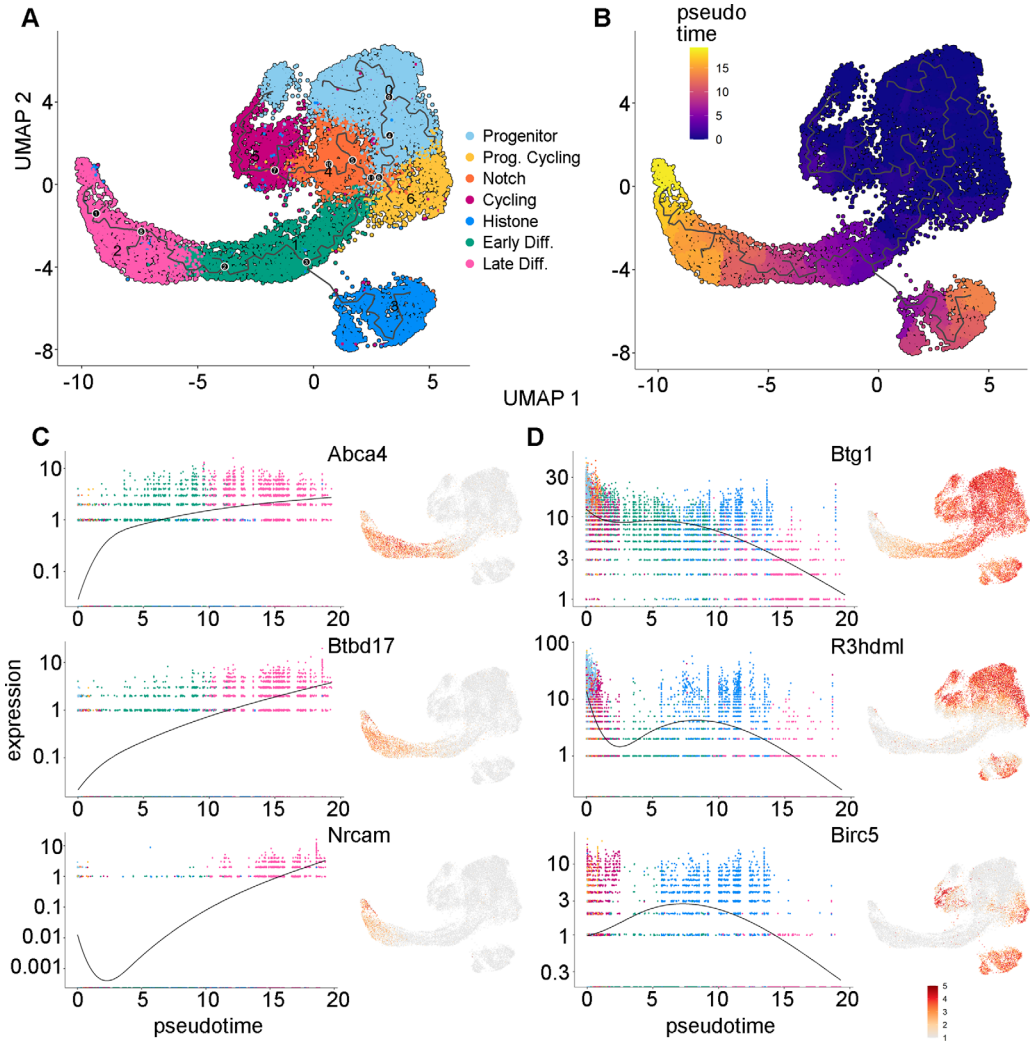

Figure 4. (**A**) The differentiation trajectory for lens epithelial cells inferred by Monocle 3, with labeled branch points (*black dots*). (**B**) UMAP representation colored by Monocle pseudotime scores. *Purple* represents cells that are earlier in pseudotime, and *yellow* indicates cells that are later in pseudotime. (**C**, **D**) For selected genes, a paired single-cell expression versus pseudotime plot (*left*) and a UMAP representation colored with relative gene expression (*right*) are shown. Plots of genes determined to be expressed later in pseudotime (**C**) and earlier in pseudotime (**D**) are shown.

Inferred Pseudotime Trajectories Supported Gene Expression–Based Cell Group Assignments

Monocle 3 was used to infer cell state changes as a function of progress along a trajectory termed "pseudotime." Pseudotime analysis confirmed the direction of differentiation states among the identified cell clusters. Monocle uses known genetic networks involved in proliferation and differentiation to unbiasedly assume temporal states of cells.[26] Starting from the Progenitor cluster, the pseudotime analysis suggested an ordering of the differentiation progression through the different cell groups to end in the Late Differentiation cluster (Figs. 4A, 4B; Supplementary Fig. S3A). Monocle also identified genes that varied or changed as a function of pseudotime. Among the genes that increased with pseudotime were *Abca4*, *Btbd17*, and *Nrcam* (Fig. 4C). The shape and attachments of LECs change throughout the process of differentiation, and this process may be aided by *Nrcam* and another late expression gene, *Pmp22*, which are both neuronal cell adhesion genes.[70] *Abca4* is also an important membrane-associated protein involved in retinal metabolism.[71] Relatively little is known about *Btbd17*, but it is also expressed in the brain and is predicted to localize in the plasma membrane.[72] Genes expressed early in pseudotime that declined in expression during development included *Btg1*, *R3hdml*, and *Birc5* (survivin) (Fig. 4D). *Btg1* is an antiproliferation factor associated with cellular differentiation and is known to be expressed in chick lens vesicles during development.[73] *R3hdml* is a TGF-β–associated signaling protein, but its specific function in the lens remains unknown.[74] *Birc5* (survivin) expression is correlated with proliferating cell subpopulations in chick lenses and is downregulated in differentiating LECs.[75] The top two expressed modules per cluster were analyzed using PantherDB GO analysis, which further functionally annotated the cell subpopulations (Supplementary Fig. S3B, Supplementary Table S1). A complete list of genes that were determined to be expressed in specific clusters is provided in Supplementary Table S2.

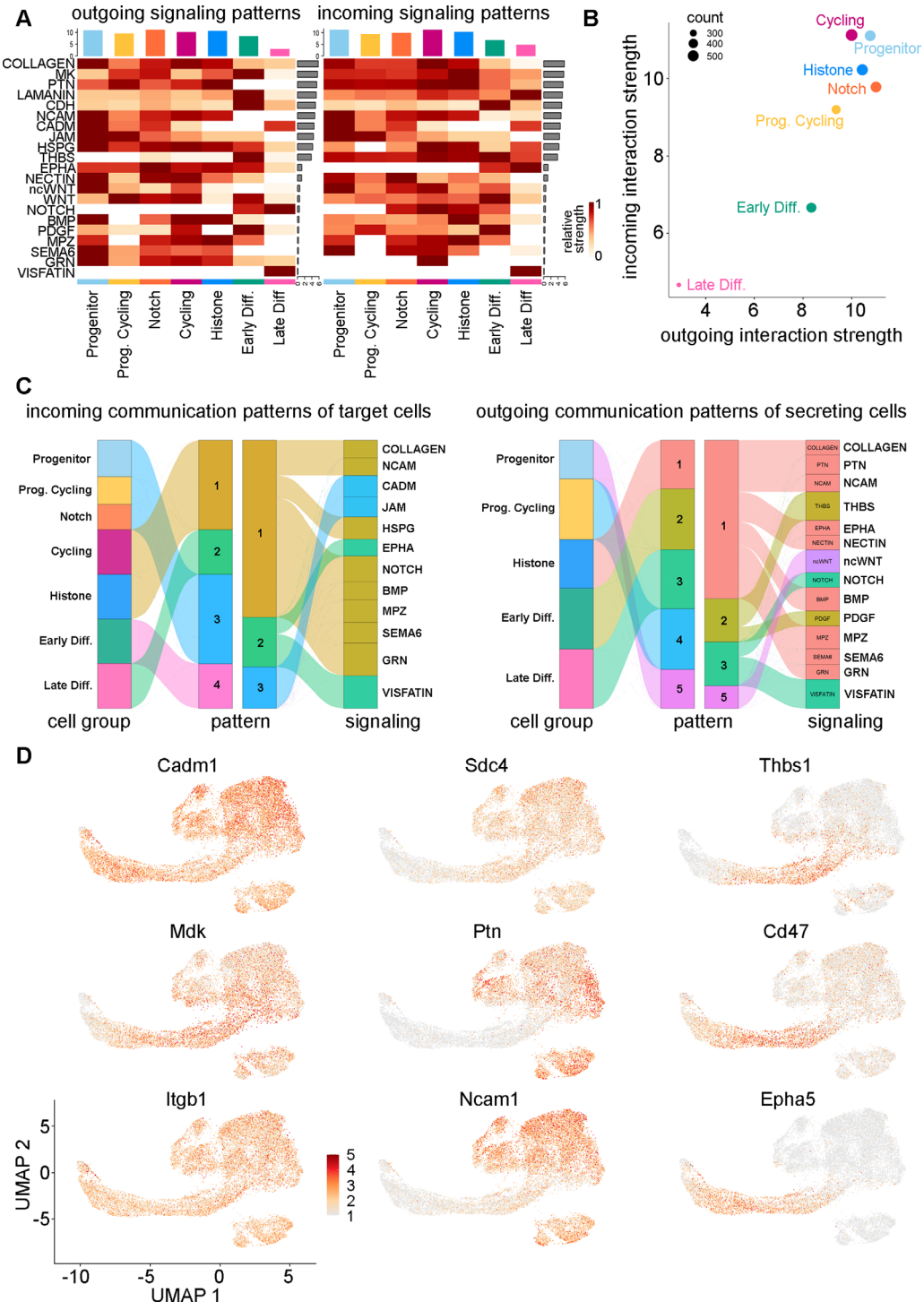

Figure 5. (**A**) CellChat net analysis heatmap of both outgoing (*left*) and incoming (*right*) significant signaling pathways per LEC subtype. Pathways are ordered by the relative strength of receptor–ligand expression and signaling communication pathway probability. (**B**) CellChat net analysis scatterplot showing the overall interaction strength of each LEC subtype to both outgoing and incoming signal strength. (**C**) River plots showing incoming (*left*) and outgoing (*right*) signaling patterns from LEC subtypes and the pathways that comprise each type of identified pattern. (**D**) UMAP representation of the expression of selected signaling molecule identified through CellChat analysis.

CellChat Identified Potential Signaling in the Different LEC Subpopulations

Signaling networks that might be active in the different LEC subpopulations were inferred and analyzed using CellChat.[28]

A general pattern that emerged was a reduction in the intensity of signaling in cell clusters identified as being in later states of differentiation (Figs. 5A, 5B), consistent with the approach toward the more inert fiber cell state. The networks that appeared to make the strongest

contributions to signaling in LECs were the collagen, midkine (MK), and pleiotrophin (PTN) signaling networks (Fig. 5A, Supplementary Fig. S4). The collagen signaling network was expressed in all clusters, but there was some differentiation of collagen expression; for example, *Col6a3* expression was upregulated in the Late Differentiating cluster (Supplementary Fig. S4C). The heparin-binding growth factors midkine (*Mdk*) and pleiotrophin (*Ptn*) were downregulated in the Late Differentiating cluster. The downstream signaling from MK and PTN receptor binding includes ERK and PI3K in other cell systems and is involved in epithelial to mesenchymal transition interactions and migration during development.[76,77] *Mdk* expression was ubiquitous in LECs, whereas *Ptn* expression disappeared in both the Early and Late Differentiating clusters (Supplementary Fig. S4C). The signaling pathways upregulated in the progenitor and cell-cycling clusters mainly included those involved in extracellular matrix (ECM) secretions, such as neural cell adhesion molecules (NCAMs), heparin sulfate proteoglycans (HSPGs), pleiotrophin, and junctional adhesion molecules (JAMs) (Fig. 5C). Pathways that were more prevalent in differentiating clusters included laminin, cadherin (CDH), thrombospondin (THBS), platelet-derived growth factor (PDGF), Notch, and visfatin. Some signaling genes, such as *Cadm1*, *Mdk*, and *Itgb1*, are expressed relatively ubiquitously in LECs, whereas other genes may be expressed uniquely during differentiation, such as *Cd47* and *Epha5* (Fig. 5D, Supplementary Fig. S4). Signaling genes upregulated earlier in pseudotime included *Ptn*, *Ncam1*, and *Sdc4*.

Discussion

The postnatal murine lens epithelium contains a pool of progenitor cells, which not only are the source of future fiber cells but also differentiate into diverse epithelial cell subtypes that are responsible for the nourishment, solute transport, and communication that the lens requires for normal growth and development.[78,79] In this study, we used scRNA-seq to provide an in-depth transcriptomic analysis of single LECs in order to probe the transcriptional and functional diversity of LEC subtypes in the early postnatal period. The data we obtained provided a snapshot of mouse lens growth and development on P2. We found that there were three major subtypes of lens epithelial cells in the mouse lens at P2: progenitor, cycling, and differentiating. These subtypes were further subdivided into seven distinct clusters based on different patterns of gene expression. The small fraction of contaminating cell types was likely derived from the tunica vasculosa lentis (TVL). Previous studies have identified the presence of mural, macrophage, and vascular endothelial cells in the TVL during this period of lens growth.[80–82]

The progenitor cell clusters displayed increased metabolic functions, including GSH synthesis pathways and lipid metabolism and synthesis. This correlates with a previous rodent lens study that identified a large increase in lipid synthesis during the first postnatal weeks.[83] Therefore, these two subpopulations of LECs could have specialized functions in maintaining the intense metabolic state during the first postnatal week of life. Interestingly, the Progenitor Cycling cluster may also be involved in progenitor self-renewal and growth of the lens during this period. Cell-cycle scoring predicted that P2 LECs had approximately a third (33.35%) of the cells undergoing the cell cycle, with approximately 20% (19.14%) in S phase, which correlates exceptionally well with analysis based on BrdU staining at P2.[10] Future studies could use scRNA-seq at other postnatal ages to track if cycling cell number decreases by P6, as was also previously documented.[10,11] Changes in the proportion of the different cell types would also be expected, because during P2 there are highly proliferative cells in both the anterior and equatorial regions, whereas by P14 these cells are almost solely concentrated in the germinative zone.[84,85]

Spatiotemporal organization of LEC subclusters could be inferred from known cell markers, as well as pseudotime analysis. Notably, high expression of *c-Maf*, *Jag1*, *Prox1*, and *Cdkn1c* (p57/KIP2) was shown throughout the early and late differentiating clusters (Supplementary Fig. S5), suggesting localization toward the lens equator. These genes are known regulators of LEC cycle exit and subsequent fiber cell differentiation.[86–88] Earlier in pseudotime, there was increased expression of *Mafb*, *Itga3*, *Cdh1*, and *Bmp7*, which are genes with established roles in lens epithelial homeostasis and development[89–91] (Supplementary Fig. S5). The upregulation of biosynthetic genes in both the Progenitor and Progenitor Cycling cluster also suggests potential functional similarities among these cell populations. Upregulation of cell-cycle genes, such as *Cdk1*, and the Seurat cell cycle scoring function were able to identify cell subpopulations undergoing the cell cycle.[67,92]

On P2, cell division in the mouse lens extends across the entire epithelium.[10,11,85] Thus, it could be hypothesized that the Progenitor and Progenitor Cycling clusters may occupy much of the anterior central zone, the Notch effector cluster could be closer to the germinative zone, and the Histone and Cycling clusters are likely anterior as well as within the germinative zone. The Early and Late Differentiating Clusters could be at the equatorial and transitional zones. Future experiments such as in situ hybridization, immunofluorescence, and spatial transcriptomics should be conducted to provide more definitive insights into the precise spatial localization of these clusters based on identified differentially expressed genes (DEGs).

Regarding cell signaling, we found that the top expressed receptor–ligand interactions originated from the collagen, midkine, and pleiotrophin pathways. The Progenitor and Cycling clusters had the most extensive signaling interactions, whereas the Differentiating clusters comparatively had comparatively lower signaling interactions. Notably, we observed heterogeneous expression of signaling molecules in cells earlier versus later in pseudotime, with some specific to cells assumed to be undergoing differentiation, including the THBS and Notch pathways. Notch signaling is known to be important in mediating epithelial to fiber cell differentiation[88] and was identified by CellChat to be upregulated in the early and late differentiating clusters only (Fig. 5). Concurrently, signaling molecules such as thrombospondin-1 also showed downregulation in the late differentiating cells relative to the early differentiating cells, which coincides with a previous study.[49] The high expression of the collagen, laminin, CDH, NCAM, cell adhesion molecule (CADM), and HSPG signaling networks is likely due to coordination of lens capsule formation or ECM remodeling and cellular migration during differentiation events. For example, the laminin and CDH networks were more prevalent in differentiating cells, whereas NCAM, CADM, JAM, HSPG, and collagen signaling events were more prevalent in progenitor and cycling cells. In addition, the gene *Itga6* (integrin subunit alpha 6) in the MK signaling system was expressed higher in the Late Differentiating cluster (Supplementary Fig. S4),

which correlates with a prior in vitro study in rats.[93] In contrast, signaling molecules such as *Ptn* were not expressed at all in the Differentiating clusters (Supplementary Fig. S4). Other signaling pathways, such as the noncanonical Wnt (ncWnt), Wnt, BMP, and myelin protein zero (MPZ), had variable signaling patterns but were mainly downregulated in the differentiating clusters. All of these pathways have established roles in lens development.[94–96] Understanding the heterogeneity of signaling in the lens epithelium is crucial for identifying how lens formation and cellular organization occur.

Some of the LEC clusters identified in our study could have distinct functions in transitioning between the proliferative and differentiating state. The Notch Effector cluster, which was also identified by pseudotime, could contain specialized cells that coordinate the differentiation versus proliferation decision.[88] In the Differentiating cell clusters, there was also an increase in ribosomal protein GO terms and expression, including *Rbm24*, which is specific to crystallin synthesis. Recently, the role of ribosomal proteins in lens translational control during development has been studied in depth, and specific translation control was found to be crucial for regulating LECs differentiation and specific protein expression.[51] In contrast, the prominent cycling histone expressing cluster remains elusive in its function. It is possible that histone remodeling could indicate a commitment to differentiation,[97,98] which is consistent with the modeling that placed this cluster later in pseudotime (Fig. 4). Alternatively, it may be linked to the transient state of high proliferation during the first postnatal week.[10] Future studies looking at histone proteins in the lens, as well as other postnatal time points, may provide insights into their functions and potential roles in differentiation commitment.

Single-cell RNA sequencing has allowed the cellular heterogeneity of postnatal LECs to be explored and has highlighted cell–cell communication networks that underlie proliferation, differentiation, and metabolism. Our findings are largely consistent with prior studies of adult human and mouse LECs. Previous scRNA-seq of human lens tissue also identified similar LEC subpopulations,[19] as did a study of adult mouse LECs.[99] This study has defined a transcriptomic atlas for the P2 mouse lens epithelium and cataloged the differential gene expression patterns of LEC subpopulations, suggesting a lineage differentiation trajectory for them. Our findings indicate that LEC heterogeneity in the developing lens is key for coordinating metabolism, self-renewal, and differentiation.

Acknowledgments

Supported by a grant from the National Institutes of Health (EY026911 to TWW).

Disclosure: **A.A. Giannone**, None; **C. Sellitto**, None; **B. Rosati**, None; **D. McKinnon**, None; **T.W. White**, None

References

1. Giannone AA, Li L, Sellitto C, White TW. Physiological mechanisms regulating lens transport. *Front Physiol*. 2021;12:818649.
2. Liu Z, Huang S, Zheng Y, et al. The lens epithelium as a major determinant in the development, maintenance, and regeneration of the crystalline lens. *Prog Retin Eye Res*. 2023;92:101112.
3. Piatigorsky J. Lens differentiation in vertebrates. A review of cellular and molecular features. *Differentiation*. 1981;19:134–153.
4. McAvoy JW, Chamberlain CG, de Iongh RU, Hales AM, Lovicu FJ. Lens development. *Eye (Lond)*. 1999;13:425–437.
5. Sikic H, Shi Y, Lubura S, Bassnett S. A stochastic model of eye lens growth. *J Theor Biol*. 2015;376:15–31.
6. Mathias RT, White TW, Gong X. Lens gap junctions in growth, differentiation, and homeostasis. *Physiol Rev*. 2010;90:179–206.
7. Tamiya S, Dean WL, Paterson CA, Delamere NA. Regional distribution of Na,K-ATPase activity in porcine lens epithelium. *Invest Ophthalmol Vis Sci*. 2003;44:4395–4399.
8. Lovicu FJ, McAvoy JW, de Iongh RU. Understanding the role of growth factors in embryonic development: insights from the lens. *Philos Trans R Soc Lond B Biol Sci*. 2011;366:1204–1218.
9. Sellitto C, Li L, Vaghefi E, Donaldson PJ, Lin RZ, White TW. The phosphoinositide 3-kinase catalytic subunit p110α is required for normal lens growth. *Invest Ophthalmol Vis Sci*. 2016;57:3145–3151.
10. Sellitto C, Li L, White TW. Connexin50 is essential for normal postnatal lens cell proliferation. *Invest Ophthalmol Vis Sci*. 2004;45:3196–3202.
11. White TW, Gao Y, Li L, Sellitto C, Srinivas M. Optimal lens epithelial cell proliferation is dependent on the connexin isoform providing gap junctional coupling. *Invest Ophthalmol Vis Sci*. 2007;48:5630–5637.
12. Lovicu FJ, McAvoy JW. Growth factor regulation of lens development. *Dev Biol*. 2005;280:1–14.
13. Bassnett S, Sikic H. The lens growth process. *Prog Retin Eye Res*. 2017;60:181–200.
14. Brewitt B, Teller DC, Clark JI. Periods of oscillatory growth in developing ocular lens correspond with cell cycle times. *J Cell Physiol*. 1992;150:586–592.
15. Farnsworth DR, Posner M, Miller AC. Single cell transcriptomics of the developing zebrafish lens and identification of putative controllers of lens development. *Exp Eye Res*. 2021;206:108535.
16. Yu J, Cheng W, Jia M, et al. Toxicity of perfluorooctanoic acid on zebrafish early embryonic development determined by single-cell RNA sequencing. *J Hazard Mater*. 2022;427:127888.
17. Liu J, Zhu M, Xu Y, et al. Autophagy-prominent cell clusters among human lens epithelial cells: integrated single-cell RNA-sequencing analysis. *BMC Ophthalmol*. 2023;23:168.
18. Shparberg R, Dewi CU, Gnanasambandapillai V, Liyanage L, O'Connor MD. Single cell RNA-sequencing data generated from human pluripotent stem cell-derived lens epithelial cells. *Data Brief*. 2021;34:106657.
19. Zhu MC, Hu W, Lin L, et al. Single-cell RNA sequencing reveals new subtypes of lens superficial tissue in humans [published online ahead of print April 14, 2023]. *Cell Prolif*, https://doi.org/10.1111/cpr.13477.
20. Yeung K, Bollepogu Raja KK, Shim YK, Li Y, Chen R, Mardon G. Single cell RNA sequencing of the adult *Drosophila* eye reveals distinct clusters and novel marker genes for all major cell types. *Commun Biol*. 2022;5:1370.
21. Tangeman JA, Rebull SM, Grajales-Esquivel E, et al. Integrated single-cell multiomics uncovers foundational regulatory mechanisms of lens development and pathology. *bioRxiv*. 2023, https://doi.org/10.1101/2023.07.10.548451.
22. Yao Y, Wei L, Chen Z, et al. Single-cell RNA sequencing: inhibited Notch2 signalling underlying the increased lens fibre cells differentiation in high myopia. *Cell Prolif*. 2023;56:e13412.

23. Satija R, Farrell JA, Gennert D, Schier AF, Regev A. Spatial reconstruction of single-cell gene expression data. *Nat Biotechnol*. 2015;33:495–502.
24. McGinnis CS, Murrow LM, Gartner ZJ. DoubletFinder: doublet detection in single-cell RNA sequencing data using artificial nearest neighbors. *Cell Syst*. 2019;8:329–337.e4.
25. Korsunsky I, Millard N, Fan J, et al. Fast, sensitive and accurate integration of single-cell data with Harmony. *Nat Methods*. 2019;16:1289–1296.
26. Trapnell C, Cacchiarelli D, Grimsby J, et al. The dynamics and regulators of cell fate decisions are revealed by pseudotemporal ordering of single cells. *Nat Biotechnol*. 2014;32:381–386.
27. Mi H, Ebert D, Muruganujan A, et al. PANTHER version 16: a revised family classification, tree-based classification tool, enhancer regions and extensive API. *Nucleic Acids Res*. 2021;49:D394–D403.
28. Jin S, Guerrero-Juarez CF, Zhang L, et al. Inference and analysis of cell-cell communication using CellChat. *Nat Commun*. 2021;12:1088.
29. Robinson ML, Overbeek PA. Differential expression of alpha A- and alpha B-crystallin during murine ocular development. *Invest Ophthalmol Vis Sci*. 1996;37:2276–2284.
30. White TW, Bruzzone R, Goodenough DA, Paul DL. Mouse Cx50, a functional member of the connexin family of gap junction proteins, is the lens fiber protein MP70. *Mol Biol Cell*. 1992;3:711–720.
31. Dahm R, van Marle J, Prescott AR, Quinlan RA. Gap junctions containing α8-connexin (MP70) in the adult mammalian lens epithelium suggests a re-evaluation of its role in the lens. *Exp Eye Res*. 1999;69:45–56.
32. Rong P, Wang X, Niesman I, et al. Disruption of *Gja8* (α8 connexin) in mice leads to microphthalmia associated with retardation of lens growth and lens fiber maturation. *Development*. 2002;129:167–174.
33. White TW. Unique and redundant connexin contributions to lens development. *Science*. 2002;295:319–320.
34. Martinez-Wittinghan FJ, Sellitto C, Li L, et al. Dominant cataracts result from incongruous mixing of wild-type lens connexins. *J Cell Biol*. 2003;161:969–978.
35. Kluger MS, Clark PR, Tellides G, Gerke V, Pober JS. Claudin-5 controls intercellular barriers of human dermal microvascular but not human umbilical vein endothelial cells. *Arterioscler Thromb Vasc Biol*. 2013;33:489–500.
36. Kalucka J, de Rooij L, Goveia J, et al. Single-cell transcriptome atlas of murine endothelial cells. *Cell*. 2020;180:764–779.e20.
37. Canfield AE, Doherty MJ, Kelly V, et al. Matrix Gla protein is differentially expressed during the deposition of a calcified matrix by vascular pericytes. *FEBS Lett*. 2000;487:267–271.
38. Mitchell TS, Bradley J, Robinson GS, Shima DT, Ng YS. RGS5 expression is a quantitative measure of pericyte coverage of blood vessels. *Angiogenesis*. 2008;11:141–151.
39. Gafencu AV, Robciuc MR, Fuior E, Zannis VI, Kardassis D, Simionescu M. Inflammatory signaling pathways regulating ApoE gene expression in macrophages. *J Biol Chem*. 2007;282:21776–21785.
40. Chen LH, Liu JF, Lu Y, He XY, Zhang C, Zhou HH. Complement C1q (C1qA, C1qB, and C1qC) may be a potential prognostic factor and an index of tumor microenvironment remodeling in osteosarcoma. *Front Oncol*. 2021;11:642144.
41. Wolf LV, Yang Y, Wang J, et al. Identification of pax6-dependent gene regulatory networks in the mouse lens. *PLoS One*. 2009;4:e4159.
42. Xie L, Chen H, Overbeek PA, Reneker LW. Elevated insulin signaling disrupts the growth and differentiation pattern of the mouse lens. *Mol Vis*. 2007;13:397–407.
43. Liu R, Blower PE, Pham AN, et al. Cystine-glutamate transporter SLC7A11 mediates resistance to geldanamycin but not to 17-(allylamino)-17-demethoxygeldanamycin. *Mol Pharmacol*. 2007;72:1637–1646.
44. Reddy VN. Glutathione and its function in the lens–an overview. *Exp Eye Res*. 1990;50:771–778.
45. Sijilmassi O. Folic acid deficiency and vision: a review. *Graefes Arch Clin Exp Ophthalmol*. 2019;257:1573–1580.
46. Lovicu FJ, McAvoy JW. Spatial and temporal expression of p57(KIP2) during murine lens development. *Mech Dev*. 1999;86:165–169.
47. Song X, Sato Y, Felemban A, et al. Equarin is involved as an FGF signaling modulator in chick lens differentiation. *Dev Biol*. 2012;368:109–117.
48. Mody AA, Millar JC, Clark AF. ID1 and ID3 are negative regulators of TGFβ2-induced ocular hypertension and compromised aqueous humor outflow facility in mice. *Invest Ophthalmol Vis Sci*. 2021;62:3.
49. Saika S, Miyamoto T, Ishida I, Barbour WK, Ohnishi Y, Ooshima A. Accumulation of thrombospondin-1 in postoperative capsular fibrosis and its down-regulation in lens cells during lens fiber formation. *Exp Eye Res*. 2004;79:147–156.
50. Collin GB, Hubmacher D, Charette JR, et al. Disruption of murine Adamtsl4 results in zonular fiber detachment from the lens and in retinal pigment epithelium dedifferentiation. *Hum Mol Genet*. 2015;24:6958–6974.
51. Nakazawa K, Shichino Y, Iwasaki S, Shiina N. Implications of RNG140 (caprin2)-mediated translational regulation in eye lens differentiation. *J Biol Chem*. 2020;295:15029–15044.
52. Qian J, Lavker RM, Tseng H. Mapping ribosomal RNA transcription activity in the mouse eye. *Dev Dyn*. 2006;235:1984–1993.
53. Shao M, Lu T, Zhang C, Zhang YZ, Kong SH, Shi DL. Rbm24 controls poly(A) tail length and translation efficiency of *crystallin* mRNAs in the lens via cytoplasmic polyadenylation. *Proc Natl Acad Sci USA*. 2020;117:7245–7254.
54. McAvoy JW. Cell division, cell elongation and the coordination of crystallin gene expression during lens morphogenesis in the rat. *J Embryol Exp Morphol*. 1978;45:271–281.
55. Landgren H, Blixt A, Carlsson P. Persistent *FoxE3* expression blocks cytoskeletal remodeling and organelle degradation during lens fiber differentiation. *Invest Ophthalmol Vis Sci*. 2008;49:4269–4277.
56. Van Leen RW, Breuer ML, Lubsen NH, Schoenmakers JG. Developmental expression of crystallin genes: in situ hybridization reveals a differential localization of specific mRNAs. *Dev Biol*. 1987;123:338–345.
57. Peek R, McAvoy JW, Lubsen NH, Schoenmakers JG. Rise and fall of crystallin gene messenger levels during fibroblast growth factor induced terminal differentiation of lens cells. *Dev Biol*. 1992;152:152–160.
58. Stein GS, Stein JL, Lian JB, Van Wijnen AJ, Wright KL, Pauli U. Modifications in molecular mechanisms associated with control of cell cycle regulated human histone gene expression during differentiation. *Cell Biophys*. 1989;15:201–223.
59. Cvekl A, Duncan MK. Genetic and epigenetic mechanisms of gene regulation during lens development. *Prog Retin Eye Res*. 2007;26:555–597.
60. He S, Limi S, McGreal RS, et al. Chromatin remodeling enzyme Snf2h regulates embryonic lens differentiation and denucleation. *Development*. 2016;143:1937–1947.
61. Vetrivel S, Tiso N, Kugler A, et al. Mutation in the mouse histone gene *Hist2h3c1* leads to degeneration of the lens vesicle and severe microphthalmia. *Exp Eye Res*. 2019;188:107632.
62. Andley UP, Naumann BN, Hamilton PD, Bozeman SL. Changes in relative histone abundance and heterochromatin in αA-crystallin and αB-crystallin knock-in mutant mouse lenses. *BMC Res Notes*. 2020;13:315.

Investigative Ophthalmology & Visual Science

63. Liu LJ, Liao JM, Zhu F. Proliferating cell nuclear antigen clamp associated factor, a potential proto-oncogene with increased expression in malignant gastrointestinal tumors. *World J Gastrointest Oncol*. 2021;13:1425–1439.
64. Riesenberg AN, Conley KW, Le TT, Brown NL. Separate and coincident expression of *Hes1* and *Hes5* in the developing mouse eye. *Dev Dyn*. 2018;247:212–221.
65. Wolf F, Sigl R, Geley S. '… The end of the beginning': cdk1 thresholds and exit from mitosis. *Cell Cycle*. 2007;6:1408–1411.
66. Tada S. Cdt1 and geminin: role during cell cycle progression and DNA damage in higher eukaryotes. *Front Biosci*. 2007;12:1629–1641.
67. Griep AE. Cell cycle regulation in the developing lens. *Semin Cell Dev Biol*. 2006;17:686–697.
68. Mahlke MA, Nechemia-Arbely Y. Guarding the genome: CENP-A-chromatin in health and cancer. *Genes (Basel)*. 2020;11:810.
69. Shin S, Zhou H, He C, et al. Qki activates Srebp2-mediated cholesterol biosynthesis for maintenance of eye lens transparency. *Nat Commun*. 2021;12:3005.
70. Beebe DC, Vasiliev O, Guo J, Shui YB, Bassnett S. Changes in adhesion complexes define stages in the differentiation of lens fiber cells. *Invest Ophthalmol Vis Sci*. 2001;42:727–734.
71. Ng ESY, Kady N, Hu J, et al. Membrane attack complex mediates retinal pigment epithelium cell death in Stargardt macular degeneration. *Cells*. 2022;11:3462.
72. Yue F, Cheng Y, Breschi A, et al. A comparative encyclopedia of DNA elements in the mouse genome. *Nature*. 2014;515:355–364.
73. Kamaid A, Giraldez F. Btg1 and Btg2 gene expression during early chick development. *Dev Dyn*. 2008;237:2158–2169.
74. Faranda AP, Shihan MH, Wang Y, Duncan MK. The aging mouse lens transcriptome. *Exp Eye Res*. 2021;209:108663.
75. Jarrin M, Mansergh FC, Boulton ME, Gunhaga L, Wride MA. Survivin expression is associated with lens epithelial cell proliferation and fiber cell differentiation. *Mol Vis*. 2012;18:2758–2769.
76. Kadomatsu K, Muramatsu T. Midkine and pleiotrophin in neural development and cancer. *Cancer Lett*. 2004;204:127–143.
77. Mitsiadis TA, Salmivirta M, Muramatsu T, et al. Expression of the heparin-binding cytokines, midkine (MK) and HB-GAM (pleiotrophin) is associated with epithelial-mesenchymal interactions during fetal development and organogenesis. *Development*. 1995;121:37–51.
78. Cvekl A, Ashery-Padan R. The cellular and molecular mechanisms of vertebrate lens development. *Development*. 2014;141:4432–4447.
79. Martinez G, de Iongh RU. The lens epithelium in ocular health and disease. *Int J Biochem Cell Biol*. 2010;42:1945–1963.
80. Ito M, Yoshioka M. Regression of the hyaloid vessels and pupillary membrane of the mouse. *Anat Embryol (Berl)*. 1999;200:403–411.
81. McMenamin PG, Djano J, Wealthall R, Griffin BJ. Characterization of the macrophages associated with the tunica vasculosa lentis of the rat eye. *Invest Ophthalmol Vis Sci*. 2002;43:2076–2082.
82. Mutlu F, Leopold IH. The structure of fetal hyaloid system and tunica vasculosa lentis. *Arch Ophthalmol*. 1964;71:102–110.
83. Cenedella RJ. Sterol synthesis by the ocular lens of the rat during postnatal development. *J Lipid Res*. 1982;23:619–626.
84. Bassnett S, Shi Y. A method for determining cell number in the undisturbed epithelium of the mouse lens. *Mol Vis*. 2010;16:2294–2300.
85. Shi Y, De Maria A, Lubura S, Sikic H, Bassnett S. The penny pusher: a cellular model of lens growth. *Invest Ophthalmol Vis Sci*. 2015;56:799–809.
86. Wigle JT, Chowdhury K, Gruss P, Oliver G. *Prox1* function is crucial for mouse lens-fibre elongation. *Nat Genet*. 1999;21:318–322.
87. Kawauchi S, Takahashi S, Nakajima O, et al. Regulation of lens fiber cell differentiation by transcription factor c-Maf. *J Biol Chem*. 1999;274:19254–19260.
88. Rowan S, Conley KW, Le TT, Donner AL, Maas RL, Brown NL. *Notch* signaling regulates growth and differentiation in the mammalian lens. *Dev Biol*. 2008;321:111–122.
89. Wawersik S, Purcell P, Rauchman M, Dudley AT, Robertson EJ, Maas R. BMP7 acts in murine lens placode development. *Dev Biol*. 1999;207:176–188.
90. Wederell ED, de Iongh RU. Extracellular matrix and integrin signaling in lens development and cataract. *Semin Cell Dev Biol*. 2006;17:759–776.
91. Pontoriero GF, Smith AN, Miller LA, Radice GL, West-Mays JA, Lang RA. Co-operative roles for E-cadherin and N-cadherin during lens vesicle separation and lens epithelial cell survival. *Dev Biol*. 2009;326:403–417.
92. Chaffee BR, Shang F, Chang ML, et al. Nuclear removal during terminal lens fiber cell differentiation requires CDK1 activity: appropriating mitosis-related nuclear disassembly. *Development*. 2014;141:3388–3398.
93. Wederell ED, Brown H, O'Connor M, Chamberlain CG, McAvoy JW, de Iongh RU. Laminin-binding integrins in rat lens morphogenesis and their regulation during fibre differentiation. *Exp Eye Res*. 2005;81:326–339.
94. Shu DY, Lovicu FJ. Insights into bone morphogenetic protein—(BMP-) signaling in ocular lens biology and pathology. *Cells*. 2021;10:264.
95. Shah R, Amador C, Chun ST, et al. Non-canonical Wnt signaling in the eye. *Prog Retin Eye Res*. 2023;95:101149.
96. Stump RJ, Ang S, Chen Y, et al. A role for Wnt/β-catenin signaling in lens epithelial differentiation. *Dev Biol*. 2003;259:48–61.
97. Bassnett S, Mataic D. Chromatin degradation in differentiating fiber cells of the eye lens. *J Cell Biol*. 1997;137:37–49.
98. He S, Pirity MK, Wang WL, et al. Chromatin remodeling enzyme Brg1 is required for mouse lens fiber cell terminal differentiation and its denucleation. *Epigenetics Chromatin*. 2010;3:21.
99. Yao Y, Wei L, Chen Z, et al. Single-cell RNA sequencing: inhibited Notch2 signalling underlying the increased lens fibre cells differentiation in high myopia. *Cell Prolif*. 2023;56:e13412.

Investigative Ophthalmology & Visual Science